A structural rationale for N-methylbicuculline acting as a promiscuous competitive antagonist of inhibitory pentameric ligand gated ion channels

Jones, Mathew J.; Dawson, Alice; Hales, Tim G.; Hunter, William N.

Published in:
ChemBioChem

DOI:
10.1002/cbic.201900680

Publication date:
2019

Document Version
Peer reviewed version

A EUROPEAN JOURNAL OF CHEMICAL BIOLOGY

CHEMBIOCHEM

SYNTHETIC BIOLOGY & BIO-NANOTECHNOLOGY

Accepted Article

Title: A structural rationale for N-methylbicuculline acting as a promiscuous competitive antagonist of inhibitory pentameric ligand gated ion channels.

Authors: William Nigel Hunter, Mathew J. Jones, Alice Dawson, and Tim G. Hales

To be cited as: *ChemBioChem* 10.1002/cbic.201900680

Link to VoR: http://dx.doi.org/10.1002/cbic.201900680

A Journal of

ChemPubSoc Europe

WILEY-VCH

www.chembiochem.org

A structural rationale for N-methylbicuculline acting as a promiscuous competitive antagonist of inhibitory pentameric ligand gated ion channels.

Mathew J. Jones,[a] Alice Dawson,[a] Tim G. Hales[b] and William N. Hunter[a]*

[a] Division of Biological Chemistry and Drug Discovery, School of Life Sciences, University of Dundee, Dow St, Dundee, DD1 5EH, Scotland UK.

[b] Division of Systems Medicine, School of Medicine, Ninewells Hospital, University of Dundee, Dundee, DD1 9SY, United Kingdom.

*w.n.hunter@dundee.ac.uk

Abstract

Bicuculline, a valued chemical tool in neurosciences research, is a competitive antagonist of specific $GABA_A$ receptors and affects other pentameric ligand gated ion channels including the glycine, nicotinic acetylcholine and 5-hydroxytryptamine type 3 receptors. We used a fluorescence quenching assay and isothermal titration calorimetry to record low micromolar dissociation constants for N-methylbicuculline interacting with acetylcholine binding protein and an engineered version called glycine-binding protein (GBP), which provides a surrogate for the heteromeric interface of the extracellular domain of the glycine receptor (GlyR). The 2.4 Å resolution crystal structure of the GBP:N-methylbicuculline complex, sequence and structural alignments reveal similarities and differences between GlyR and the $GABA_A$ receptor bicuculline interactions. N-methylbicuculline displays a similar conformation in different structures but adopts distinct orientations enforced by interactions and steric blocks with key residues and plasticity in the binding sites. These features explain the promiscuous activity of bicuculline against the principal inhibitory pentameric ligand gated ion channels in the CNS.

Introduction

The alkaloid bicuculline competitively antagonises activation of the inhibitory $GABA_A$ receptor ($GABA_AR$) by the native agonist γ-aminobutyric acid.[1-3] This natural product has played a seminal role in early studies of synaptic transmission in particular helping to characterise the role of γ-aminobutyric acid as a neurotransmitter.[3,4] Subsequently, concerns linked to compound instability, poor solubility and activities on other receptors were raised.[5,6] Bicuculline has poor aqueous solubility, and is highly

susceptible to hydrolysis of the lactone moiety, with a half-life of 45 minutes at physiological pH, to produce inactive bicucine.[7] These complicating factors can be overcome by using the N-methylbicuculline salts (Figure 1A), which are more stable and soluble.[2,8,9] However, an issue previously described is the haphazard reporting of which variant has been used in experiments.[2] A point we will mention again. The alkaloid is also active against related pentameric ligand gated ion channels (pLGICs) including the other inhibitory system, the glycine receptor (GlyR),[10] the excitatory serotonin and nicotinic acetylcholine receptors (nAChR). This complication is compounded by activity against the unrelated calcium-activated potassium channels.[11,12] A range of IC_{50} values for activity against different receptors is presented in Supplementary material Table S1.

Bicuculline is GABA competitive and interacts with the orthosteric site of pLGICs.[3] The compound also acts as an inverse agonist, inhibiting $GABA_A$-receptor subtype activity that is independent of agonist binding to the orthosteric site.[13,14] Since receptor specific residues, at key positions influence pLGIC ligand specificity and affinity [15-17] we sought to understand how this semi-rigid compound was able to antagonise the transmission of inhibitory potentials in the distinctive GlyR and $GABA_AR$ systems. These receptors consist of intracellular, transmembrane and extracellular domains.[15,16] The acetylcholine-binding protein from *Aplysia californica* (*Ac*AChBP) shares sequence identity and structural homology with the extracellular domain (ECD) of pLGICs, and has been exploited as a surrogate system.[18-20] We engineered an AChBP derivative called glycine binding protein (GBP) as a surrogate for the physiologically relevant β[+]/α[-] heteromeric interface of GlyR.[21] The orthosteric binding site is formed at the interface of two subunits with three loops (termed A-C) contributed from the principal [+]-subunit, and the [-]-complementary subunit donates another four loops, D-G (Figure 1B-D). We have characterised the interactions between N-methylbicuculline, also termed (-)-bicuculline methiodide with *Ac*AChBP and GBP. Affinity and thermodynamic data are derived from a tryptophan fluorescence quenching assay and isothermal titration calorimetry (ITC). We attempted to co-crystallize N-methylbicuculline with wild type *Ac*AChBP and variants generated by site-directed mutagenesis to investigate aspects of GlyR and $GABA_AR$ activity to no avail. We did however obtain a crystal structure of the N-methyl derivative with GBP at 2.4 Å resolution that provides a description of interactions in the neurotransmitter or orthosteric binding site and infers how the ligand modulates GlyR activity. Comparisons with $GABA_AR$ amino acid sequences and a structure derived by cryogenic-electron microscopy (cryo-EM)[22] inform a discussion about the promiscuous activity of the alkaloid against this sub-group of the pLGIC family.

Results and Discussion

Bicuculline, and the more stable N-methyl derivative are primarily hydrophobic, and semi-rigid with a single C-C bond about which rotation defines the alignment of the dioxolophthalide and dioxoloisoquinolium moieties with respect to each other (Figure 1A). The solvent accessible surface area of N-methylbicuculline is around 520 Å^2 with a polar surface area of only about 70 Å^2. There are six oxygen atoms capable of accepting hydrogen bonds and with an estimated p*K*a of 14.7, under physiological conditions bicuculline is protonated and a hydrogen bond can be donated by the quaternary ammonium. The N-methyl derivative lacks this hydrogen bond donating capacity.

There is a requirement to use DMSO to dissolve the ligand at a concentration required to investigate binding. Given the potential complications of using this solvent[23] we first ascertained how it might affect GBP. We characterized the thermal stability of GBP by recording the inflection point of a melting curve in different levels, 0 to 10%, of DMSO. This indicated that 2% DMSO could be appropriate. Next, a time course experiment indicated that for binding assays the 2% DMSO level was not deleterious to the sample. Control experiments were carried for ITC and fluorescence measurements allowing us to take into account the presence of DMSO in the binding assays.

The binding of N-methylbicuculline to GBP and *Ac*AChBP was investigated using a fluorescence quenching assay exploiting the presence of Trp164 in the binding site and gave dissociation constant (K_d) values of 8.7 ± 0.5 μM and 1.2 ± 0.1 μM respectively (Supplementary material Figure S1). An orthogonal ITC assay resulted in thermodynamic dissociation constant (K_D) values of 29.6 ± 10.0 μM and 4.7 ± 1.6 μM (Supplementary material Figure S2). We note however, that the molar ratios for N-methylbicuculline binding (mol ligand/mol pentamer) derived from the ITC data are not 5:1 as would be expected for a single site binding event but rather 4:1 for the association with *Ac*AChBP and nearly 12:1 with GBP. In comparison, use of a ^{3}H-strychnine competition binding assay gave IC_{50} values of 5-6 μM for bicuculline acting on the GlyR[24,25] whilst electrophysiology experiments recorded values in the range 169 to 300 μM for N-methylbicuculline.[26,27] When tested against mammalian nAChRs, again using an electrophysiology assay, bicuculline retained antagonist properties with IC_{50} values in the range 12 to 34 μM, moreover with Hill coefficients demonstrated to be close to unity.[28] It has been noted, using ITC,[29] that certain ligands for example carbamylcholine bind the pentameric *Ac*AChBP with a molar ratio of 2.5:1 yet with no evidence for cooperativity or allosteric transitions in this protein. Carbamylcholine displays a similar affinity for *Ac*AChBP, 7.6 ± 0.4 μM[29] as N-methylbicuculline and the reason for the low molar ratio is unclear. Other ligands (e.g. acetylcholine) fit the 5:1 ratio. Our ITC data were derived from curves with low c values of between 3 and 7. Whilst not optimal such values are considered acceptable[30] with the proviso that some caution should be exercised when drawing conclusions. In our case, we note a consistency in the data derived using two distinct biophysical assays. We note also that the binding of N-methylbicuculline

and bicuculline occurs with comparable affinity to *Ac*AChBP, GBP and to members of the pLGIC superfamily. Contrary to observations with *Ac*AChBP, the molar ratio with GBP may indicate the presence of multiple binding sites.

The crystal structure of the GBP: N-methylbicuculline complex has a pentamer in the asymmetric unit with each orthosteric site occupied by a single molecule of ligand (Figure 1B, Supplementary material Table S1, Figure S3) and no evidence for any other binding site. Of course, the conditions under which crystals are obtained are different from those employed for binding studies. The subunits are labelled A-E, and ligands are assigned to the subunit that forms the principal side of the binding site. We imposed non-crystallographic symmetry (NCS) in the initial refinement of the complex but on observing deviations released these restraints in the binding site. This in particular applies to key residues, Tyr205 and Tyr212, in different orthosteric sites and will be discussed below. The electron density is well defined for most of the polypeptide chains, indeed in places sufficiently so that dual rotamers were modelled. However, at the periphery of the binding sites involving subunits B-E, the electron density is diffuse for part of loop C and several residues could not be modelled reliably. Gly207 and Thr208 were omitted in subunits B-E, Lys206 also from B, C and E. Our observation is consistent with conformational flexibility previously noted for this part of the binding site and which is relevant to function.[15, 20] The crystallographic order of the ligands differs as indicated by variability in definition of the electron density and the average *B*-factors. Our interpretation of the crystallographic data is a model with two similar poses of the ligand in a ratio 3:2, which identify the orientation of the ligand bound to a site that possesses a degree of conformational flexibility. Pose I is observed for ligands B, D, E and pose II for A and C. The *B*-factors, or displacement parameters, indicate that the most ordered subunits are A and B with average B-factors of 43.5 and 40.3Å^2 respectively. The most ordered ligand displaying pose I is at the interface formed between subunits B[+]/C[-] with an average *B*-factor of 65.2 Å^2 and real-space correlation coefficient (RSCC) value of 0.90. The most ordered pose II is at the A[+]/B[-] interface with an average *B*-factor of 95.7 Å^2 and RSCC 0.88. The solvent accessible surface area (SASA) values are similar for each pose varying between 519 and 532 Å^2 and when bound to GBP approximately 60% of the SASA is lost. We describe the details of the most ordered pose I since this correlates with the highest level of crystallographic order (Figure 2) and comment briefly on pose II (Supplementary material Figure S4).

A feature, deep in the orthosteric binding site, is the well-ordered arrangement of aromatic residues Trp164, Tyr212, and Tyr72 which create a π-electron rich environment to interact with the positively charged methylated amine. Such an interaction is an important feature of pLGIC ligand complexes.[17,18,31] In addition there are van der Waals interactions between ligand and protein involving these residues. The side chain of Glu162, juxtaposed between Trp164 and Tyr212, is directed to the quaternary amine making

an electrostatic contribution to ligand binding. On the complementary side, the phthalide part of the ligand makes van der Waals contacts to Phe53, Arg74, Met133 and Ser135. The latter two residues act like a wedge between the phthalide and isoquinolium components and, together with Tyr212 from the other subunit, help to orient the ligand. The dioxoloisoquinolium occupies a depression between loops B and C of the principal subunit. Here, there are van der Waals interactions with main chain atoms of the tripeptide segment Val165, Tyr166, and Ser167 and side chains atoms of Tyr205, Glu210, and Tyr212. The side chain of Val125 also makes van der Waals interactions to this end of the ligand and here the position of Arg96 is noted.

The dioxolo group associated with the phthalide can accept two hydrogen bonds donated by Arg96 on the complementary side and a protonated Glu210 on the principal side. Although the geometry is not ideal the distance of 3.3 Å suggests that the dioxolo group attached to the isoquinolium may accept a hydrogen bond donated by Arg74 NE. The other oxygen is solvent accessible, 4.1 Å from the hydroxyl group of Tyr205 on the flexible loop C. The remaining two hydrogen bond acceptor groups are from the lactone. These oxygen atoms are 3.1 and 3.2 Å from a well-ordered water molecule (*B*-factor 31 Å^2) with an environment and geometry suggestive of a bifurcated hydrogen bond. The water in turn donates a hydrogen bond to the carbonyl of Trp164 then accepts a hydrogen bond from another highly ordered water, (*B*-factor 31 Å^2). An overlay of the *Ac*AChBP nicotine complex (PDB code 5O87)[18] with the structure reported here indicates that the first water maps to the position of the pyridine N of nicotine. The second water represents a highly conserved hydration point, which forms hydrogen bonds with main chain groups of residues Ile123 and Ile135 in *Ac*AChBP, Ser135 in GBP, and to another water that continues a solvent network through to the surface of the protein (data not shown). This ordered solvent structure is consistently noted in high-resolution structures of AChBP ligand complexes.[15,20]

Considering pose II; the conformation of the ligand is preserved with a similar orientation of the dioxolophthalide and dioxoloisoquinolium entities with respect to each other, and the quaternary amine occupies the same relative position in the orthosteric site (Supplementary material Figures S4 and S5A). Pose II participates in similar interactions as described for pose I, e.g. the key cation-π interaction of the quaternary amine with the protein. However, the orientation differs slightly in that for pose II the ligand pivots, as a rigid body, about the amine and the dioxoloisoquinolinium is placed closer to Phe53 and Tyr72, further from Met133. Although an ordered water molecule occupies the same position as that discussed above, the lactone is now too far for a hydrogen bond to form. The dioxolophthalide is positioned further from the tripeptide segment Val165, Tyr166, and Ser167 on the principal side. The side chains of Tyr205 and Tyr212 adopt different rotamer conformations compared to those involved in binding pose I, and accommodate this slight rigid body adjustment whilst maintaining van der Waals interactions with the ligand. The hydrogen bonds with Arg96 and Glu210 however, are lost.

We considered first if the GBP:N-methylbicuculline complex was representative of how a GlyR β[+]/α1[-] orthosteric site might interact with the ligand. The alignment of sequences and the crystal structure of the human GlyR-α3 homomer in complex with strychnine (PDB code: 5CFB),[32] were used to inform on similarity between the orthosteric sites of GBP and the GlyR β[+]/α1[-] combination (Figure 3). Arg96, a contribution from the complementary side of the orthosteric site, is not usually considered as part of the binding site and is not included in Figure 3. This residue corresponds to Asp112 in GlyR-α1. The contributions of fifteen residues in GBP that interact with N-methylbicuculline have been described earlier. Seven of the residues are strictly conserved in the relevant human GlyR subunits (Phe53, Arg74, Ser135, Glu162, Tyr166 and Tyr205, Tyr212). A further four involve conservative substitutions (Met133Leu, Trp164Phe, Tyr72Phe, Ser167Thr). The differences involve Arg96Asp, Val125Arg and Val165Gly substitutions, and Glu210. The Val165Gly substitution is unlikely to be significant since the residue forms van der Waals interactions with the ligand using the main chain. Glu210 and Tyr212 are on the flexible loop C with some uncertainty about which residues on the GlyR β-subunit they would align with. If GBP Tyr212 aligns with GlyR-β Tyr253 as we think most likely (Figure 3), then the interactions with the ligand and loop C would be conserved. Tyr252 could also provide stabilizing associations including a hydrogen bond donor group to interact with the ligand. That leaves Val125 to consider together with Arg96. These residues are close together on adjacent β-strands. In human GlyR-α1 they correspond to Arg147 and Asp112 respectively and both are conserved in GlyR-α3. A superposition with the GlyR-α3 crystal structure indicates that the Arg96Asp difference places the acidic group directed away from the binding site, but critically, the Val125Arg substitution places the guanidinium groups at the same position to interact with the ligand (Supplementary material Figure S6).

Alkaloids carrying a tetrahydroisoquinoline core can induce convulsions.[10] We were particularly interested in features relevant to recognition of that part of N-methylbicuculline. There are nine residues that interact with the dioxoloisoquinolinium entity (Phe53, Tyr72, Arg74, Met133, Ser135, Glu162, Trp164, Tyr205 and Try212). Six of these are strictly conserved, and three represent conservative substitutions in GlyR (Tyr72Phe, Met133Leu, and Trp164Phe). This suggests that the N-methylbicuculline complex is indeed representative of how isoquinolium antagonists bind a heteromeric GlyR orthosteric site to effect competitive antagonism.

Figure 3 also presents alignments of GBP with three $GABA_AR$ subunits, this being the other inhibitory pLGIC. Again, Arg96, which corresponds to Arg112 in human $GABA_A$-α1, is not shown. The recent cryo-EM structure of the complex between bicuculline and human $GABA_A$–$[\alpha1]_2[\beta3]_2[\gamma]$ receptor[22] offered the opportunity for comparison and further analysis. First a comment; there is an inconsistency in the description of what was used to derive the structure in PDB entry 6HUK.[19] The publication and PDB

entry describe bicuculline methochloride being used but the coordinates and chemical diagram indicate bicuculline in both β3[+]/α1[-] sites and that is used in our comparisons. We calculate RSCC values of 0.84 and 0.81 for the ligands, comparable to values in our crystal structure.

The conformation of the semi-rigid molecule is essentially identical between the two complex structures (Supplementary material Figure S5B). An overlay of two subunits that create an orthosteric site, in each protein, positions the quaternary ammonium groups within 0.8 Å. The environment of the cationic group is similar in the two structures. The acidic Glu162 of GBP is strictly conserved as Glu180, and the cluster of aromatic residues also maintained. These are Phe53, Tyr72, Trp164, Tyr205 and Tyr212 in GBP, which correspond to Phe73, Phe92, Tyr182, Phe225, and Tyr230 respectively in $GABA_AR$ (Figure 4). A significant difference involves Thr108 in GBP, which is Tyr122 in the $GABA_AR$-β3 sequence. The increase in size of the side chain places the tyrosine hydroxyl into the cation binding pocket helping to orient the ligand.

However, although the interactions between the receptors and the cationic group are conserved the orientation of the ligands in the orthosteric sites is different (Figure 4). The isoquinolium entities occupy a similar position in the binding site but are orthogonal to each other and their distinct orientations are accompanied by concerted adjustments of side chain rotamers for several of the aromatic residues deep in the binding site. This alteration of the isoquinolium, together with a tilt about the ammonium places the dioxolophthalide components of the ligands in completely different positions. In the case of GBP, this part of the ligand is placed over towards the principal loop C on one side and the complementary side loop E on the other. In the $GABA_AR$ structure the dioxolophthalide component is directed towards the other end of the orthosteric site, near loop G (Figure 4B). The nature of the amino acid at two positions on the complementary side and one on loop C of the principal side appear to contribute to the observation of two distinct orientations. In GBP, the positions of Arg96 and Val125, discussed above, align to Arg112 and Arg147 in the $GABA_AR$ orthosteric site. The juxtaposition of the two arginine residues in the $GABA_AR$ orthosteric site places the side chain of Arg147 to hydrogen bond with Tyr230 from loop C on the principal side to, in effect, provide a steric block preventing the dioxolophthalide from adopting the orientation observed when in complex with GBP. The crystal structure of bicuculline itself has been determined.[33] Superposition of this structure on that of the models derived from the protein complex structures indicates that in isolation a different conformation is observed with the two ring systems rotated about 90° relative to each other (Supplementary material Figure S5C). Our comparisons therefore suggest that although the semi-rigid alkaloid can adopt different conformations, only one is observed when the ligand binds to inhibitory pLGICs. However, this conformation can be present in two distinct orientations in distinct

neurotransmitter binding sites so explaining the promiscuous activity of bicuculline on these inhibitory ion channels.

The ρ-class $GABA_AR$, also known as the $GABA_C$ receptor is insensitive to bicuculline[34] and we sought to test our understanding by exploring this aspect of ion channel pharmacology. The alignment of the human $GABA_AR$-ρ1 sequence with the sequences and structures described is presented in Figure 3. A previous attempt to promote a gain of function in $GABA_AR$-ρ1with respect to bicuculline antagonism was based on molecular modelling, site directed mutagenesis, and electrophysiology.[34] The combination of Tyr127Ser (loop D) and Phe159Tyr (loop A) substitutions, and the tripeptide Phe261-Tyr262-Ser263 (loop C) changed to a dipeptide Val-Phe gave the largest increase in bicuculline sensitivity though still at least an order of magnitude reduced from the $GABA_A$-β3[+]/α1[-] system. The introduction of the serine would be predicted to open up space behind a conserved arginine (Arg125 in $GABA_AR$-ρ1, Arg74 in GBP) and allow it to act to interact with bicuculline. The Phe159Tyr change would place the hydroxyl group to form stabilising interactions with the quaternary ammonium and create an environment to interact with the cationic group similar to position of Tyr122 on the β3 subunit of the $GABA_A$ β3[+]/α1[-] structure. The changes to a tripeptide on loop C may simply provide space to accommodate the ligand or to place the phenylalanine to mimic Phe226 of the β3 structure. That these changes only produce a limited gain of function indicates that other features must be important.

Our comparisons drew attention to the role of loop C and Phe53 in GBP, conserved as Phe73 in the $GABA_AR$-α1 subunit. In the $GABA_A$-β3[+]/α1[-] orthosteric binding site Phe73 aligns to Gln104 in the ρ1 sequence. The presence of a polar glutamine would remove van der Waals interactions between the phenyl group and both dioxolo groups of the ligand and is likely to prevent bicuculline binding in the orientation noted in the cryo-EM structure. Whilst loop C is more highly conserved with the α1 sequence, which is on the principal side not the complementary one. It is difficult without structural data on the ρ1 receptor to be certain about what happens with loop C, but the presence of a bulky Trp267 on the ρ1 subunit could potentially block access to the ligand. Further data would however be required to more completely address the selectivity issues of the $GABA_A$-ρ1 receptor.

Conclusions

In summary, N-methylbicuculline binds to GBP with low micromolar affinity, comparable to that displayed against members of the pLGIC family (Supplementary material Table S1). The crystal structure of the complex with GBP has been elucidated with the ligand modelled in two similar poses that represent an orientation of the compound in the binding site. Comparisons of sequences and structures identify

significant similarities between GBP and GlyR orthosteric sites and we conclude that the orientation of N-methylbicuculline is representative of how the alkaloid acts as a competitive antagonist against GlyR. When bicuculline binds the human $GABA_AR$, the natural product displays the same molecular conformation as when bound to GBP, with conservation of interactions involving the quaternary ammonium group. However, the molecule adopts a different orientation in the binding site. This observation is likely a consequence of only a few specific amino acid differences between the two proteins. The binding of this promiscuous competitive antagonist appears to be driven by the charge-π interaction of the quaternary ammonium with the protein and van der Waals interactions that can be accommodated by flexibility inherent in the pLGIC orthosteric sites.

Experimental Section

Protein Production: A recombinant source of *Ac*AChBP (Uniprot ID Q8WSF8) and GBP with a C-terminus tobacco etch virus cleavage site and His_6 tag were produced in baculovirus infected *Sf*9 insect cells using the Bac-to-Bac expression system (Thermo-Fisher). Suspension High Five insect cells, cultured in Express Five medium plus 100 U/ml penicillin/streptomycin and 2 mM L-glutamine (Thermo-Fisher), were used for protein production. Typically, $15x10^5$ cells/ml were infected with 5% of baculovirus carrying the appropriate gene and incubated at 27 °C in shaking flasks for 48 hours before being harvested by centrifugation (1500g, 10 minutes, 12°C followed by 4000g, 10 minutes, 12°C). The proteins are secreted out to the media and using the Sartojet system with a 10 kDa cut-off Sartocon Slice filter (Sartorius), the media was exchanged for buffer A (50 mM Tris-HCl, 250 mM NaCl pH 7.5) and the sample concentrated. The protein solution was applied to a 5 ml Ni^{2+} HisTrap column (GE Life Sciences) equilibrated in buffer A for immobilised metal anion chromatography. The column was washed with 15 column volumes of buffer A + 7.5% buffer B (50 mM Tris-HCl, 250 mM NaCl, 800 mM imidazole pH 7.5) then the product eluted over 30 column volumes using a combination of a stepped and linear gradient of buffer B. A native-page gel (Supplemental material Figure S7A) identified the presence of monomer, the desired pentamer, and a higher order multimer, possibly a dimer of pentamers. For size exclusion chromatography, a Superdex 200 10/300 GL column was equilibrated overnight in buffer A then samples loaded and run over 1.5 column volumes (Supplemental material Figure S7B). The retention time of each peak was recorded, and the molecular weight deduced from a previously determined calibration curve. Use of stain free SDS-PAGE gels (Bio-Rad, Supplemental material Figure S7C)) allowed us to confirm the presence of the protein and fractions corresponding to the desired pentameric assembly were pooled and samples concentrated using 10 kDa centrifugal concentrators (Pall).

Crystallographic Analysis: GBP at a concentration of 4 mg/mL in buffer A (50 mM Tris-HCl pH 7.5, 150 mM NaCl) was incubated with 2 mM bicuculline methiodide (Sigma-Aldrich; 20 mM stock in buffer A, 20% DMSO), diluted in buffer A, for 1 hr before crystallisation trials using commercially available PEGS (Qiagen) and JCSG (Molecular Dimensions) screens. Sitting-drops (final volume 0.2 µL) comprised a 1:1 mix of protein and reservoir (a volume of 50 µL was used in the plates) were prepared with a Rigaku Phoenix automated dispenser and incubated at 18 ^{o}C for one month. A suitable crystal (rectangular prism, 0.7 x 0.25 x 0.25 mm) appeared from a condition with a reservoir of 0.2 M ammonium formate and 20% (w/v) PEG 3350. The crystal was immersed in liquid nitrogen, then placed under a stream of nitrogen gas at around -170 ^{o}C and diffraction data collected with a Rigaku M007HF copper-anode generator, Varimax Cu-VHF optics, Saturn 944HG+ CCD detector and AFC-11 4-axis partial χ goniometer. The data were integrated with XDS,[35] scaled with AIMLESS[36] and the structure was solved via molecular replacement with PHASER,[37] exploiting the already refined structure of GBP with glycine (PDB code: 5OAN).[19] Multiple rounds of automated restrained refinement were completed using REFMAC5,[38] interspersed with model adjustment based on inspection of electron and difference density maps in COOT.[39] NCS restraints were employed at the onset of the refinement but when real differences became apparent these were released. Ligand models and restraints were generated with the GRADE server [Global Phasing - http://grade.globalphasing.org/cgi-bin/grade/server.cgi]. Ligands, water molecules and chloride ions, together with several dual rotamers were incorporated into the model. Asn91 is glycosylated and N-acetyl-D-glucosamine was modeled onto several subunits at this position. Several residues that were not well defined by the electron density were omitted from the model. All the above software was available through the CCP4 suite.[40] All structural figures were prepared using Pymol (pymol.org) and annotated in Microsoft PowerPoint. Crystallographic statistics are in Supplementary material Table S2.

Assessing the effect of DMSO on thermal stability of GBP: Solutions of GBP (0.5 mg/mL) were prepared with varying concentrations of DMSO (0-10%) and incubated at room temperature for 5 mins. The inflection point (Ti) of the unfolding transition as the samples are heated was determined based on the ratio of fluorescence at 350:330 nm on a Nanotemper Tycho NT.6 instrument. Experiments were carried out in triplicate, then the mean and standard deviation of each measurement determined and plotted (Supplementary material Figure S8). A further assessment was carried out in which GPB was incubated with 2% DMSO at room temperature and the Ti determined at 15 min intervals over 45 mins. Experiments were conducted in triplicate, then the mean and standard deviation of each was calculated. These values were then compared to the 0% DMSO control. The data indicated that over 45 mins, the time period required for the biophysical assays, there is no determinantal effect from a 2% level of DMSO on protein stability.

Fluorescence Quenching Assay: Stock solutions of 10 µg/mL GBP and *Ac*AChBP were prepared, along with a 4 mM stock of bicuculline methiodide (100 mM stock in DMSO), in buffer A. Data were collected on a LS-55 PerkinElmer spectrometer with the detector sensitivity set to 750 V. Protein samples (volume 2 mL) were excited at a wavelength of 280 nm, and emissions between 300-400 nm were monitored. Additions of 1-2 µl of the N-methylbicuculline stock were dispensed, each followed by mixing, for a total of 20 µl. Experiments were carried out in triplicate and the percentage change in fluorescence was calculated. Control measurements adding buffer to the protein solutions whilst matching the concentration of DMSO were conducted. These were then subtracted from the percentage change in fluorescence to provide a correction for the presence of DMSO (Supplementary material Figure S9).

Isothermal Titration Calorimetry: Experiments were carried out using a PEAQ-ITC (MicroCal, Malvern Panalytical) at 25 ^{o}C. GBP and *Ac*AChBP solutions, at a concentration of 40 µM were prepared by dialysis against buffer A at 4 ^{o}C overnight, then DMSO was added to match that in the titrant. Bicuculline methiodide (concentration 2 mM, 2% DMSO) was prepared in the same buffer. The injection needle acted as a paddle stirring the cell contents at 750 rpm. An initial injection of 0.4 µL was followed by twelve 3 µL injections at 3 minute intervals. Data were analysed using the software supplied by the manufacturer assuming a one binding site model with mean composite controls: buffer-buffer, buffer-protein, ligand-buffer considered. Titrations were conducted in triplicate. The controls, original traces plus derived titration curves and parameters with average values are in Supplementary material Figure S10 and Table S3. Representative data are presented in Figure S2E.

Sequence and Structure Alignments: Sequences for GlyR (Uniprot codes: α_1 P23415 and β P48167) and $GABA_A$ (Uniprot codes: α1 P14867, β3 P28472, ρ1 P24046) receptors, were extracted from Uniprot and aligned using Clustal Omega on the Jalview platform.[41] GBP (PDB code: 5OBH) and the $GABA_A$ receptor (PDB code: 6HUK) files were retrieved from the Protein Data Bank and superimposed in COOT, by SSM superimpose. Images were then produced in Pymol, after using the align function to obtain an optimal overlay of the two structures, with ten cycles of refinement.

Acknowledgements

Funded with support from a Wellcome Trust PhD studentship and equipment grant [094090]. We thank Dr. Paul Fyfe and Dr Paul Davis for many useful discussions.

Conflict of Interest

The authors declare no conflict of interests.

Key words: acetylcholine binding protein . alkaloid . competitive antagonist . crystal structure . $GABA_A$-receptor . glycine receptor

References

[1] D. R. Curtis, A. W. Duggan, D. Felix, G. A. R. Johnston, *Nature* 1970, **226**, 1222-1224.

[2] G. A. R. Johnston, P. M. Beart, D. R. Curtis, C. J. A. Game, R. M. McCulloch, R. M. Maclachlan, *Nature New Biol.* 1972, **240**, 219-220.

[3] G. A. R. Johnston, *Br. J. Pharmacol.* 2013, **169**, 328-336.

[4] D. R. Curtis, A. W. Duggan, D. Felix, G. A. R. Johnston, *Brain Res.* 1971, **32**, 69-96.

[5] D. W. Straughan, M. J. Neal, M. A. Simmonds, G. G. S. Collins, R. G. Hill, *Nature* 1971, **233**, 352-354.

[6] V. Seutin, S. W. Johnson, *Trends Pharmacol. Sci.* 1999, **20**, 268-270.

[7] R. W. Olsen, M. Ban, T. Miller, *Brain Res.* 1976, **102**, 283-299.

[8] S. F. Pong, L. T. Graham, Jr., *Brain Res.* 1972, **42**, 486-490.

[9] J. Krall, T. Balle, N. Krogsgaard-Larsen N, T. E. Sørensen, P. Krogsgaard-Larsen, U. Kristiansen, B. Frølund, *Adv. Pharmacol*. 2015 **72**, 201-227

[10] P. Li, M. Slaughter, *Vis. Neurosci.* 2007 **24**, 513-521.

[11] R. Khawaled, A. Bruening-Wright, J. P. Adelman, J. Maylie, *Pflügers Arch.* 1999, **438**, 314-321.

[12] D. Strøbaek, T. D. Jørgensen, P. Christophersen, P. K. Ahring, S. P. Olesen, *Br. J. Pharmacol.*, 2000, **129**, 991-999.

[13] S. Ueno, J. Bracamontes, C. Zorumski, D. S. Weiss, J. H. Steinbach, *J. Neurosci.* 1997**, 17**, 625-634.

[14] M. R. McCartney, T. Z. Deeb, T. N. Henderson, T. G. Hales, *Mol. Pharmacol*. 2007**, 71**, 539-548.

[15] M. Nys, D. Kesters, C. Ulens, *Biochem. Pharmacol.* 2013, **86**, 1042-1053.

[16] D. Lemoine, R. Jiang, A. Taly, T. Chataigneau, A. Specht, T. Grutter, *Chem. Rev.* 2012, **112**, 6285-6318.

[17] P. J. Corringer, F. Poitevin, M. S. Prevost, L. Sauguet, M. Delarue, J. P. Changeux, *Structure* 2012, **20**, 941-956.

[18] T. K. Sixma, A. B. Smit, *Annu. Rev. Biophys. Biomol. Struct.* 2003, **32**, 311-334.

[19] A. Shahsavar, M. Gajhede, J. S. Kastrup, T. Balle, *Basic Clin. Pharmacol. Toxicol.* 2016, **118**, 399-407.

[20] L. Sauguet, A. Shahsavar, M. Delarue, *Biochim. Biophys. Acta* 2015, **1850**, 511-523.

[21] A. Dawson, P. Trumper, J. Oliveira de Souza, H. Parker, M. J. Jones, T. G. Hales, W. N. Hunter, *IUCrJ* 2019, **6**, 1014-1023.

[22] S. Masiulis, R. Desai, T. Uchański, I. S. Martin, D. Laverty, D. Karia, T. Malinauskas, J. Zivanov, E. Pardon, A. Kotecha, J. Steyaert, K. W. Miller, A. R. Aricescu, *Nature* 2019, **565**, 454-459.

[23] A. Tjernberg, N. Markova, W. J. Griffiths, D. Hallén, *J. Biomolec. Screen.* 2006, **11**, 131-137.

[24] A. Goldinger, W. E. Müller, *Neurosci. Lett.* 1980, **16**, 91-95.

[25] J. C. Marvizón, J. Vázquez, M. G. Calvo, F. Mayor, A. R. Gómez, F. Valdivieso, J. Benavides, *Mol. Pharmacol.* 1986, **30**, 590-597.

[26] N. Tokutomi, M. Kaneda, N. Akaike, *Br. J. Pharmacol.* 1989, **97**, 353-360.

[27] H. Sun, T. K. Machu, *Eur. J. Pharmacol.* 2000, **391**, 243-249.

[28] A. Demurom, E. Palma, F. Eusebi, R. Miledi, *Neuropharmacology* 2001, **41**, 854-861.

[29] P. H. Celie, S. E. van Rossum-Fikkert, W. J. van Dijk, K. Brejc, A. B. Smit, T. K. Sixma, *Neuron* 2004, *41*, 907-914.

[30] W. B. Turnbull, A. H. Daranas, *J. Am. Chem. Soc.* 2003, **125**, 14859-14866.

[31] W. Zhong, J. P. Gallivan, Y. Zhang, L. Li, H. A. Lester, D. A. Dougherty, *Proc. Natl. Acad. Sci. U. S. A.* 1998, **95**, 12088-12093.

[32] X. Huang, H. Chen, K. Michelsen, S. Schneider, P. L. Shaffer, *Nature* 2015, **526**, 277-280.

[33] C. Gorinsky, D. S. Moss, *J Cryst. Mol. Struct* 1973, *3*, 299-307.

[34] J. Zhang, F. Xue, Y. Chang, *Mol. Pharmacol.* 2008, **74**, 941-951.

[35] W. Kabsch, *Acta Crystallogr. D* 2010, **66**, 125-132.

[36] P. R. Evans, G. N. Murshudov, *Acta Crystallogr. Sect. D: Struct. Biol.* 2013, **69**, 1204-1214.

[37] A. J. McCoy, R. W. Grosse-Kuntsleve, P. D. Adams, M. D. Winn, L. C. Storoni, R. J. Read, *J. Appl. Crystallogr.* 2007, **40**, 658-674.

[38] G. N. Murshudov, P. Skubák, A. A. Lebedev, N. S. Pannu, R. A. Steiner, R. A. Nicholls, M. D. Winn, F. Long, A. A. Vagin, *Acta Crystallogr. Sect. D: Struct. Biol.* 2011, **67**, 355-367.

[39] P. Emsley, K. Cowtan, *Acta Crystallogr. Sect. D: Struct. Biol.* 2004, **60**, 2126-2132.

[40] M. D. Winn, C. C. Ballard, K. D. Cowtan, E. J. Dodson, P. Emsley, P. R. Evans, R. M. Keegan, E. B. Krissinel, A. G. W. Leslie, A. McCoy, S. J. McNicholas, G. N. Murshudov, N. S. Pannu, E. A. Potterton,

H. R. Powell, R. J. Read, A. Vagin, K. S. Wilson, *Acta Crystallogr. Sect. D: Struct. Biol.* 2011, **67**, 235-242.

[41] A. M. Waterhouse, J. B. Procter, D. M. Martin, M. Clamp, G. J. Barton, *Bioinformatics* 2009, **25**, 1189-1191.

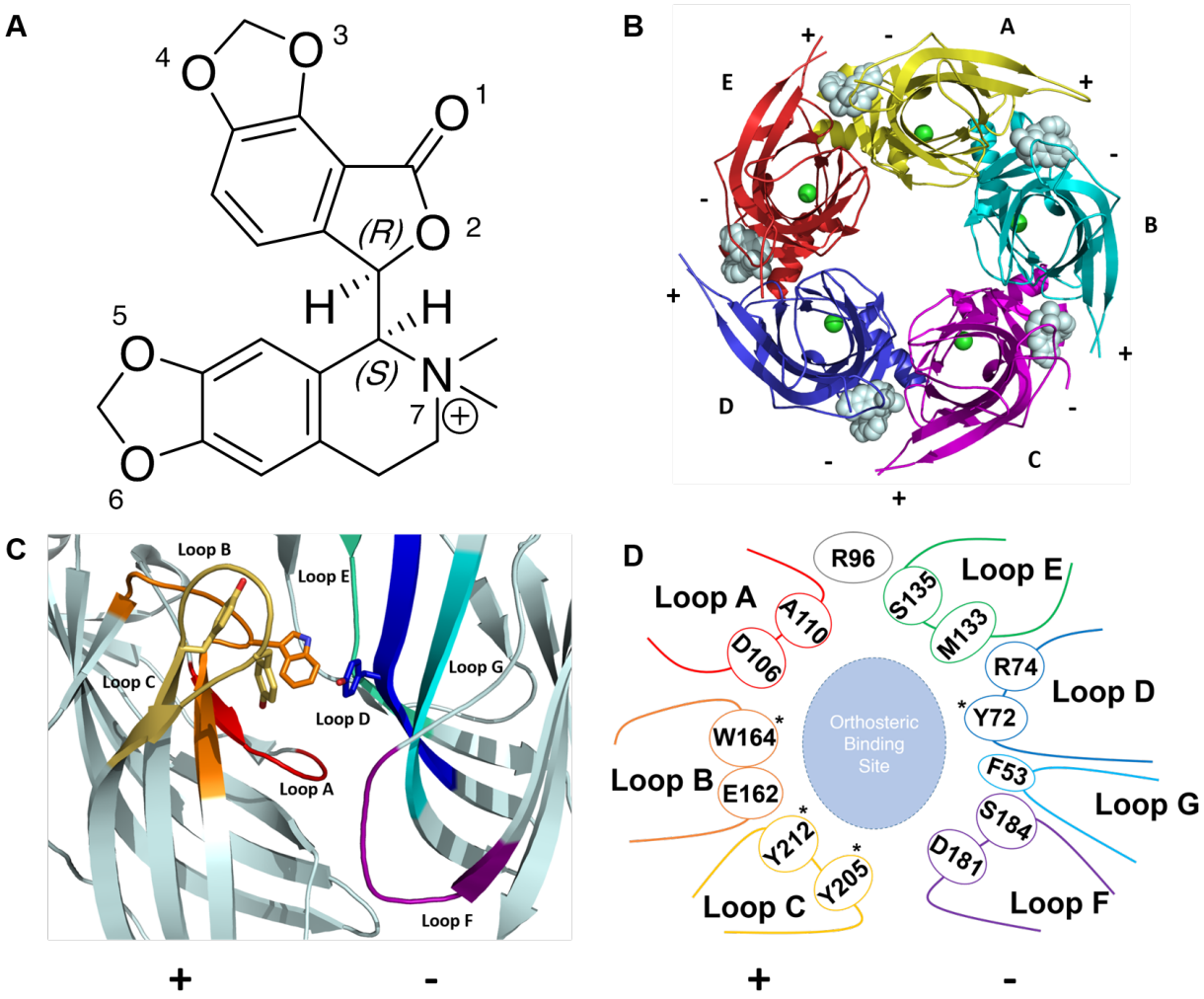

Figure 1. (A) The structure of (-)-N-methylbicuculline. N and O atoms are numbered. (B) Ribbon diagram of GBP showing the five subunits (labelled A to E and in different colours) and the principal [+] and complementary [-] sides at the orthosteric binding sites. N-methylbicuculline (grey van der Waals spheres) occupies each site. Chloride (green spheres) bound in each subunit are shown. (C) Molecular image of an orthosteric binding pocket of GBP showing, the principal subunit donating loops A (red), B (orange), C (yellow) and the complementary subunit contributing loops D (blue), E (blue), F (purple), G (cyan). The aromatic cage side chains (Tyr72, Trp164, Tyr205 and Tyr212) are shown as sticks with C positions colored according to which loop they belong with. (D) Schematic representation of the GBP binding site, starred residues are responsible for the aromatic cage. Arg96 is not associated with any of the loops.

10.1002/cbic.201900680

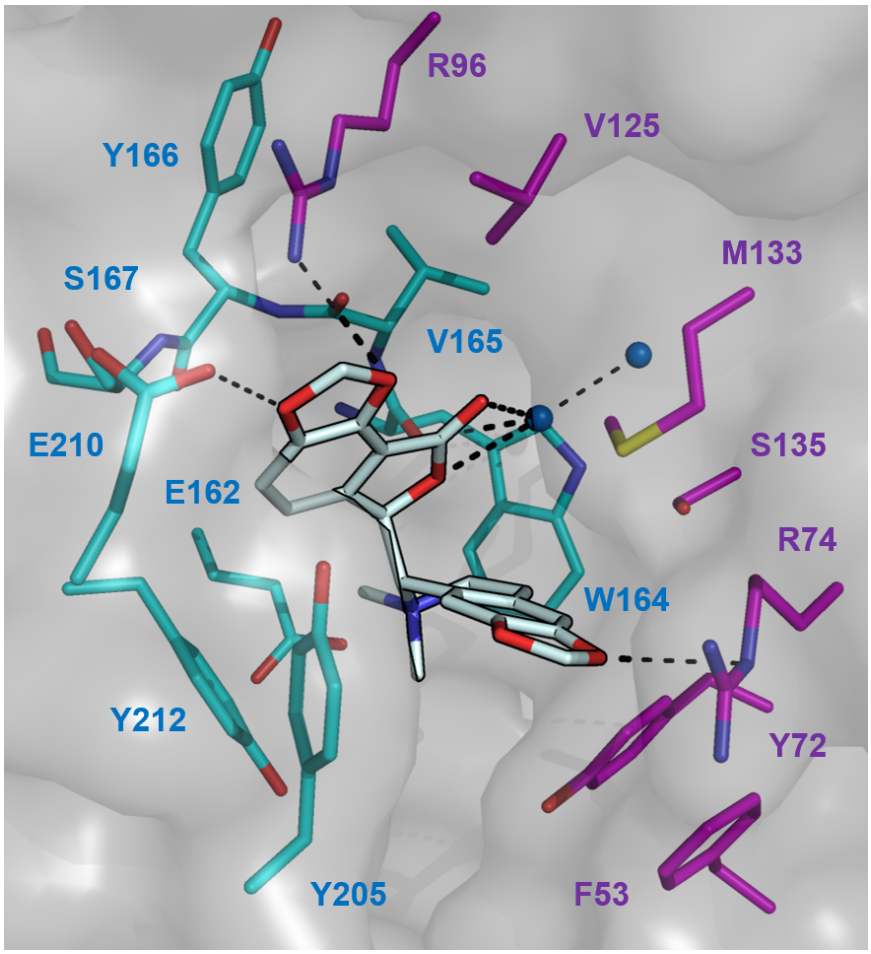

Figure 2. N-methylbicuculline binding to GBP. The ligand, pose I, is shown as sticks with C positions silver. The protein surface is presented as a semi-transparent van der Waals surface (grey) Residues from the [+]-principal (C positions cyan) and [-]-complementary (C positions magenta) subunits are shown. N, O, S positions are blue, red and yellow respectively. Two water molecules are depicted as blue spheres. Putative hydrogen bonds are represented as black dashed lines.

	PRINCIPAL [+]			COMPLEMENTARY [-]			
Loop	A	B	C	D	E	F	G
	105	161	204	72	123	181	51
GBP	P D I T A A	F E S W V Y S	H Y K G T G E P Y I	Y E R Q R W	I A V V T H D G S V M F S	D L S S	G F F L Q
	124	184	229	91	145	205	70
GlyRα1	P D L F F A	L E S F G Y T	H Y N – T G – K F T	**F L R Q Q W**	**L L R I S R N G N V L Y S**	**Q V A D**	**N I F I N**
	141	201	246	106	106	222	85
GlyRβ	**P D L F F A**	**L E S F G Y T**	**Y Y K G T G – Y Y T**	F L R Q K W	L L F I F R D G D V L V S	Q L E K	N I F I N
	124	184	230	91	145	207	71
GABAα1	P D T F F H	F G S Y A Y T	V Q S S T G E Y V V	**F F R Q S W**	**L L R I T E D G T L L Y T**	**V V A E**	**D I F V T**
	119	179	224	87	140	200	66
GABAβ3	**P D T Y F L**	**I E S Y G Y T**	**V F A – T G – A Y P**	Y F Q Q Y W	M I R L H P D G T V L Y G	V T G V	N I D I A
	156	216	261	123	177	237	102
GABAρ1	P D M F F V	I E S Y A Y T	F Y S S T G – W Y N	Y L R H Y W	M L R V Q P D G K V L Y S	L K T D	D V Q V E

Figure 3. Sequence alignment of segments involved in creating the orthosteric binding sites of GBP, two human GlyR forms (α1 and β) and three $GABA_A$-R forms (α1, β3, ρ1). The loops are identified and split into principal and complementary sides. Residues in red were engineered into AChBP to create GBP, a

surrogate for a heteromeric GlyR orthosteric site and are key to ligand interactions. Residues that contribute to heteromeric binding sites are shown in bold.

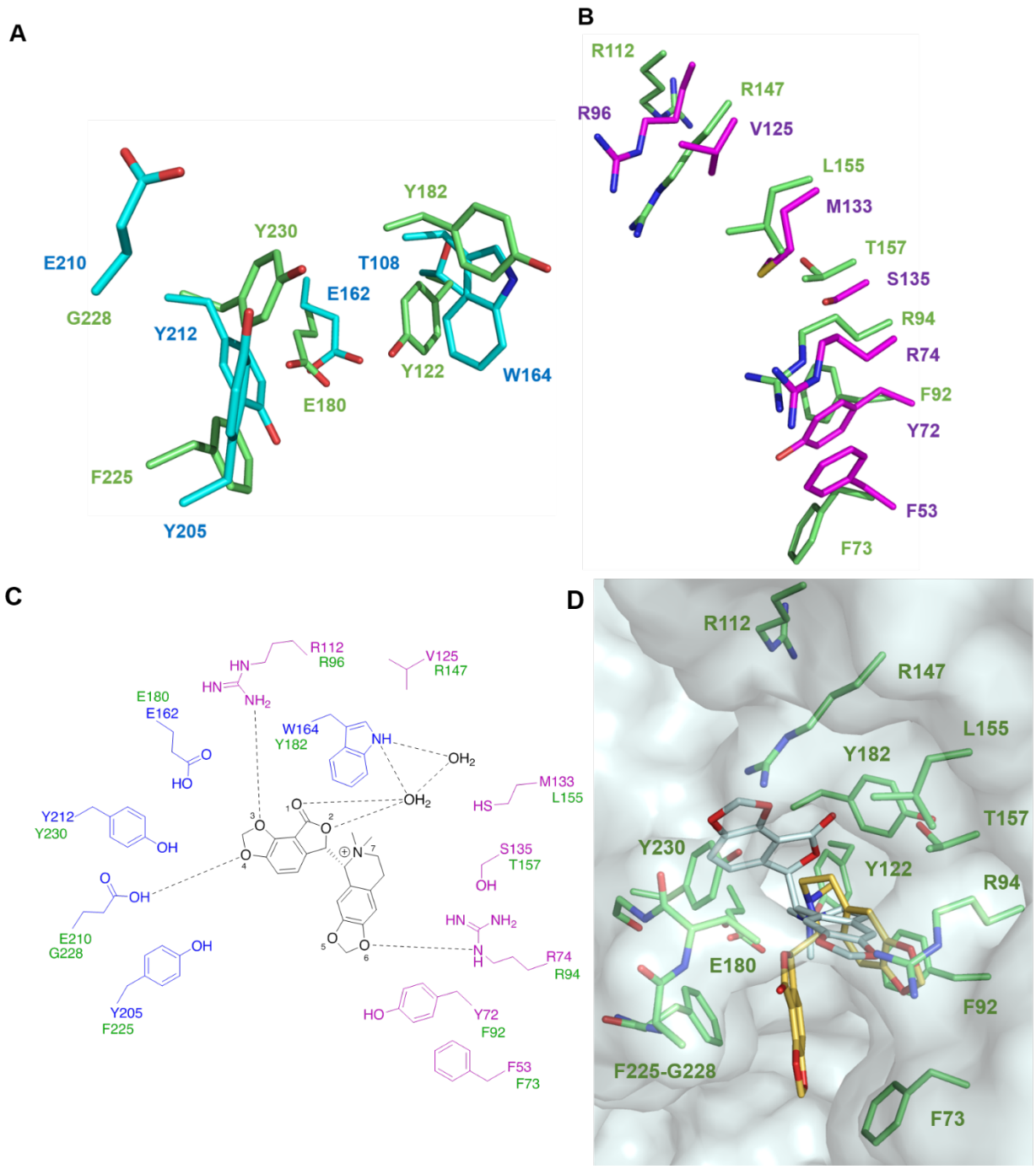

Figure 4. Comparison of key residues of GBP and $GABA_A$-R. The alignment of the structures is based on a least-squares overlay with the cryo-EM structure (PDB code 6HUK). (A) The principal subunits with

GBP residue side chains shown as sticks with C positions colored cyan and O red, the corresponding $GABA_A$-R residues shown with C positions green. (B) The complementary subunits with GBP C positions colored magenta. (C) A schematic diagram of pose I in the GBP N-methylbicuculline complex. The corresponding residues in $GABA_A$-R are labelled in green. (D) An overlay to show the distinct orientations of N-methylbicuculline bound to GBP (silver C) and bicuculline bound to $GABA_A$-R (yellow C) in the $GABA_A$-R orthosteric site. $GABA_A$-R is shown as a semi-transparent van der Waals surface (grey) with key residues in the binding pocket shown as in parts (A) and (B). The numbering of the $GABA_A$-R residues is taken from the Uniprot entries (α1 P14867 and β3 P28472).